Molecular Crystals and Liquid Crystals

ISSN: 1542-1406 (Print) 1563-5287 (Online) Journal homepage: http://www.tandfonline.com/loi/gmcl20

Flexo-Dielectro-Optical Spectroscopy as a Method of Studying Nanostructured Nematic Liquid Crystals

M. Vijay Kumar, S. Krishna Prasad, Y. Marinov, L. Todorova & A. G. Petrov

To cite this article: M. Vijay Kumar, S. Krishna Prasad, Y. Marinov, L. Todorova & A. G. Petrov (2015) Flexo-Dielectro-Optical Spectroscopy as a Method of Studying Nanostructured Nematic Liquid Crystals, Molecular Crystals and Liquid Crystals, 610:1, 51-62, DOI: 10.1080/15421406.2015.1025205

To link to this article: http://dx.doi.org/10.1080/15421406.2015.1025205

Mol. Cryst. Liq. Cryst., Vol. 610: pp. 51–62, 2015

ISSN: 1542-1406 print/1563-5287 online
DOI: 10.1080/15421406.2015.1025205

Taylor & Francis
Taylor & Francis Group

Flexo-Dielectro-Optical Spectroscopy as a Method of Studying Nanostructured Nematic Liquid Crystals

M. VIJAY KUMAR,[1] S. KRISHNA PRASAD,[1] Y. MARINOV,[2] L. TODOROVA,[2] AND A. G. PETROV[2,*]

[1]Centre for Nano and Soft Matter Sciences, Jalahalli, Bangalore, India
[2]Institute of Solid State Physics, Bulgarian Academy of Sciences, Sofia, Bulgaria

The method of flexo-dielectro-optical spectroscopy was initially developed to study the spectra of the linear and quadratic electro-optic response of continuous nematic liquid crystal layers as a function of the frequency of the applied electric field at low frequencies (0.1–10000 Hz) [1]. Subsequently, it was applied to the microconfined PDLC system [2].

*In the present study a nanoconfined nematic system of 4-*n*-heptyl cyanobiphenyl liquid crystal (7CB) containing hydrophilic silica nanoparticles (Aerosil 300) was investigated. The method was implemented by a lock-in detection of the 1st and 2nd harmonic of transmitted laser light through a nanonematic layer subjected to a.c. electric field, the results of which are compared with those for pure 7CB. The optical spectra recorded at various temperatures in the nematic phase of pure and nanostructured samples are presented along with data from static and dynamic measurements of the Freedericksz transition.*

The data so obtained contain information about liquid crystal disorder induced by the nanoparticles both in the bulk and in the nanoscale vicinity of each particle or network of paticles. They are interpreted in terms of two subsystems model, and dimensions of bulk and nanostructured domains evaluated.

Keywords nanostructured nematic; silica nanoparticles; Freedericksz transition; statics and dynamics; low frequency modulation spectra of transmitted light; 1st and 2nd harmonic

Introduction

Studies on the influence of externally imposed geometrical restrictions on liquid crystalline properties have been attracting significant attention in recent times [3]. The geometrical restrictions could be imposed by confining liquid crystals (LC) in membranes such as Anopore, Nuclepore, etc. having a regular matrix or in an irregular network like in the case of aerogels. The ensuing disorder realized in these situations can also be obtained by dispersing certain particles like aerosil in the LC medium. The reason for this choice being that aerosil particles, having ~ 7 nm diameter, have their surfaces surfaces decorated to achieve hydrophilic or hydrophobic interactions. The advantage of these particles is

*Address correspondence to A. G. Petrov, Institute of Solid State Physics, Bulgarian Academy of Sciences, 72 Tzarigradsko chaussee, 1784 Sofia, Bulgaria. E-mail: director@issp.bas.bg

Color versions of one or more of the figures in the article can be found online at www.tandfonline.com/gmcl.

that mere variation of the particle concentration allows control and fine tuning of the random disorder. Calorimetric and X-ray scattering measurements have been extensively used to investigate LC- aerosil systems, particularly employing the homologues of the alkyl cyano biphenyl family [4–13], and show that for low concentration or density of aerosil (denoted ρ_a) the system behaves as a soft gel with sharp phase transitions whereas at higher concentrations the transitions are smeared out.

Electric properties of nanocomposites of nematic liquid crystals containing nanoparticles have attracted much interest ever since 1991 [14,15], when it was demonstrated by employing mixtures containing cyanobiphenyl compounds that these systems can provide bistable electrooptical displays based on light scattering and without the need for polarizers. In this work we look at both the linear and non-linear flexo response of the system to an applied electric field. The frequency-dependent measurements have been performed on both pure and the nano (aerosil)-filled heptyl cyanobiphenyl compound, which was chosen as the host since comparisons can be made with the literature available on this substance.

2. Experimental

2.1. Preparation of nanocomposites

For the confinement studies, hydrophilic aerosil particles from Degussa Corporation, Aerosil 300 (kindly given to us by Mr. Vikas Rane of d-hindia Ltd, Mumbai) having a diameter of ~ 7 nm and specific surface area of 300 m^2/g, were used. The surfaces of the particles are capped with silanol groups that are responsible for the fragile hydrogen bonded network formed by the spheres when present in a fluid medium. Before the preparation of mixtures, the aerosil was degassed and dried at 300°C for about 15 h. 7CB was used in this study because it exhibits nematic phase in broad temperature interval including room temperature. Mixtures of aerosil in 7CB were prepared by two different methods i.e., (a) simple physical mixing and (b) standard solution method. In the former method, appropriate weights of aerosil and LC materials were physically stirred while maintaining the temperature of the system at ~ 10°C above the clearing point (i.e., the nematic–isotropic transition point). For the solvent mixing method, the two samples were dispersed in a large quantity (5 ml) of methanol added. The whole mixture was sonicated for about 30 minutes to obtain a good dispersion of the aerosil in the medium. While keeping the temperature at 60°C the solvent was evaporated slowly over a period of 1 h. The prepared sample was kept under vacuum for 24 h to ensure complete evaporation of methanol.

Aerosil mixtures are usually characterized in terms of the aerosil density defined as $\rho_a = m_a/V_{LC}$, where m_a is the mass of aerosil and V_{LC} is the volume of liquid crystal (as the density of the LC is ~ 1 g cm^{-3}, ρ_a can be taken to be m_a/m_{LC}). Investigations have been carried out on mixtures with $\rho_a = 0.03$g cm^{-3} as well as on pure 7CB.

2.2. Methods

The differential scanning calorimetric (DSC) experiments were performed using a model DSC8000 calorimeter (Perkin Elmer) operating on the principle of power-compensation. These experiments were performed on the bulk LC material as well as on the aerosil composites. For this purpose the samples, having a nominal mass of 3 mg, were loaded into aluminium pans and the DSC thermograms were taken in nitrogen atmosphere.

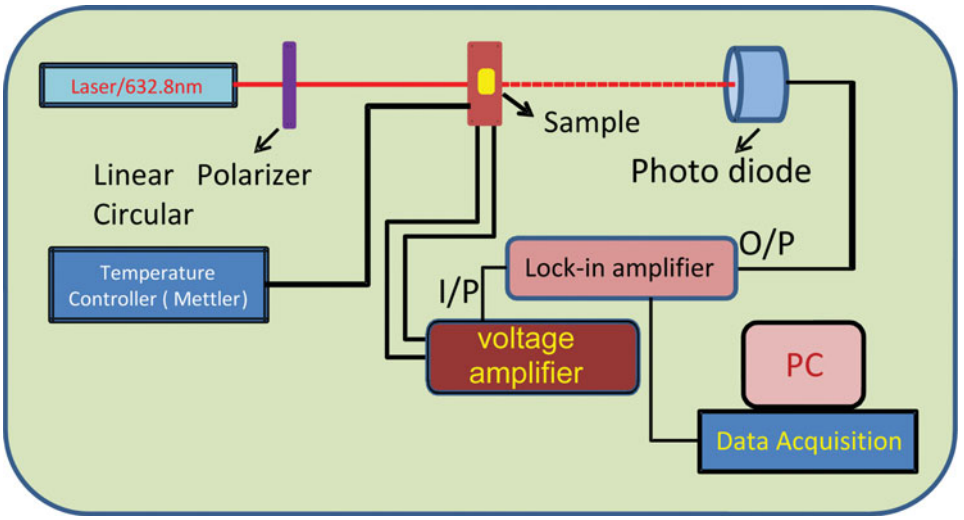

Figure 1. Schematic diagram of the experiment

For the measurements involving application of electric field, the samples were taken in a sandwich cell made up of ITO coated glass substrates with a low ($<10\Omega/cm^2$) sheet resistivity. Prior to the assembly of the cell, the glass plates were treated with a polyimide solution and unidirectionally rubbed to impart uniform alignment of the molecules parallel to the substrate surface. The samples were filled into the cell in the isotropic phase by capillary action.

A schematic diagram of the apparatus used for the experiments is shown in Figure 1. The laser beam from a HeNe laser was polarized (linear or circular polarization), and the intensity transmitted through the sample was collected using a high speed pin diode. Usually, circular polarization was implemented with nanofilled samples, in order to average effects due to random local axes distribution. The driving electric field was sourced from the oscillator output of a wide frequency digital built-in function generator (Picoscope 6242) amplified using a high-fidelity high voltage amplifier (TREK 50). The outputs of the oscillator as well as the photodiode were acquired through a 16-bit high sampling rate oscilloscope, the digital output of which was collected on a PC. The high bit resolution and the sampling rate enabled reliable Fast Fourier Transform operation to be performed on the

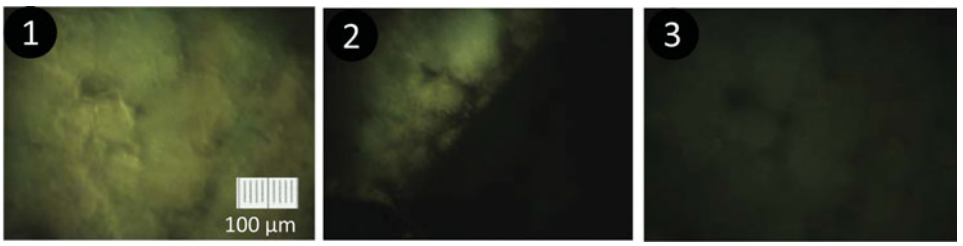

Figure 2. Dark field images of 25 μm thick nanofilled nematic layer (7CB+ 3%A300); from left to right: liquid crystal (plate 1) and isotropic (plate 3) phase, plate 2 showing phase transition between the two. Objective 25x. Size of images is 530 $\times$ 400 μm.

data and extraction of the harmonic signals. At low driving frequencies, the FFT operation permitted observation of a discernable signal even up to the 6th harmonic.

Alternatively, a computer-driven SR830 lock-in amplifier provided simultaneously the AC excitation with variable (sweep) frequency and the registration of 1st or 2nd harmonic of the modulated transmitted light, both amplitude and phase. Computer control of the AC amplitude permitted the application of pulses (wave packets of desired frequency) as well. The temperature of the sample was varied using a Mettler hot stage and the associated controller.

3. Results

3.1. Polarizing and Dark Field Microscopy

Images of nanodoped 7CB in crossed polars are obtained with NU-2 universal microscope (Zeiss Jena), using pancratic condenser. Dark field images are obtained by cardioid oil immersion condenser. Interestingly, dark field images are visible not only in nematic, but also in isotropic phase. In the last case these are very fine clouds on a dark background, presumably due to the faint scattered light from the hydrogen bonded network of nanoparticles.

3.2. Differential scanning calorimetry of 7CB+A300

Across the nematic-isotropic transformation, while the pure LC exhibits a single peak, the aerosil composite shows two peaks, albeit the lower temperature one is very weak. Two peak-profiles seen across N-I [3,13,16,17] are understood as doubling of the phase transition due to a crossover from a random-dilution regime, where the silica gel couples to the scalar part of the nematic order parameter, to a low-T random-field regime, where the coupling induces distortions in the director field. [17].

It may be recalled here that twin peak profiles across the N-I transformation have also been observed when an organogelator is used instead of aerosil particles [18a]. The gelator, itself a mesogen, gives rise to the formation of fibre bundles in the gel state. Thus an alternate explanation for the twin-peak profile could be that the transition sequence could actually be: Isotropic sol-anisotropic sol (regular nematic)-anisotropic gel (nematic gel), i.e., in the region between the two peaks the material is actually in the neamtic sol state. Notably, the appearance of twin-peak profiles is also reported in the cases of LC colloids with metal nanoparticles (MNP), but without any gelation [18b,c]. In these cases while the random field crossover phenomenon mentioned above is possible, it could be argued that a surface transition, separated from a bulk transition, is responsible for the observations [18c]. Considering the phenomenon to be uniform irrespective of whether the *particles* added are nanoparticles of the gelating or the non-gelating kind, or nanofibres, we can state the following. In all the cases, the bulk transition is caused by molecules which are away from the particle surfaces and thus not influenced by them. The second transition arises due to the molecules which are bonded to (physically or otherwise), or even in the immediate proximity of the particles. The LC ordering of such "surface" LC molecules could be, dependending on the particle surface, different from the "bulk" region. The net result would be two thermal anomalies, one corresponding to the bulk and the other caused by the surface molecules. Finally, a point that should be borne in mind is that at the concentration and temperature studied by us the nematic phase of the composite is a soft gel.

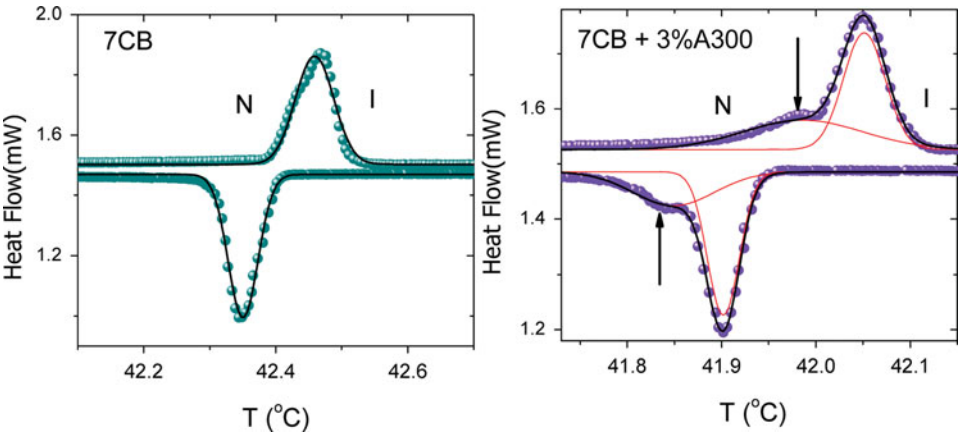

Figure 3. DSC thermograms for pure (left panel) and nanofilled 7CB (right panel). The black line represents the fit of the data to a single Gaussian expression for 7CB, and a sum to two Gaussians for the composite. The red lines in the right panel depict the individual contributions of the two peaks.

3.3. Pure 7CB: Freedericksz transition

First electro-optical studies of filled nematics and of hydrogen-bonded aerosil systems were reported in [14] and [15] by employing cyano based compounds. Our electro-optical curves of the Freedericksz transition in planar 7CB layers at several temperatures in the nematic phase are given in Figure 4. The transition was driven by 1 kHz ac voltage, with variable amplitude. For convenience, transmitted laser light through the LC cell between crossed polarizers was chopped at 404 Hz, and its amplitude was recorded from the lock-in amplifier.

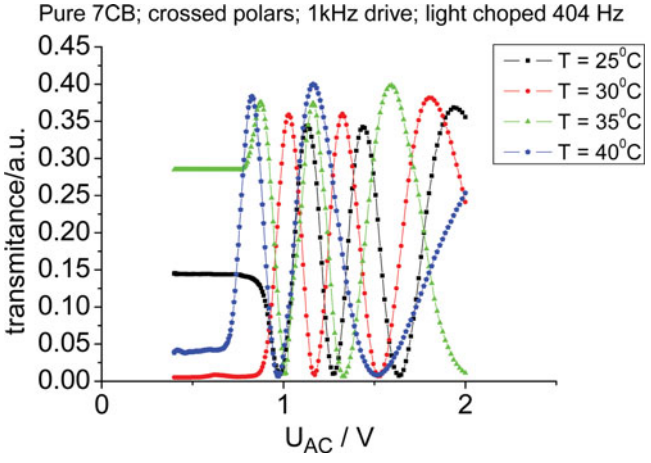

Figure 4. Transmittance vs. voltage curves of pure 7CB in the nematic phase, demonstrating the temperature dependence of the Freedericksz threshold (as shown on Figure 7). AC driving voltage of 1kHz. Crossed polars.

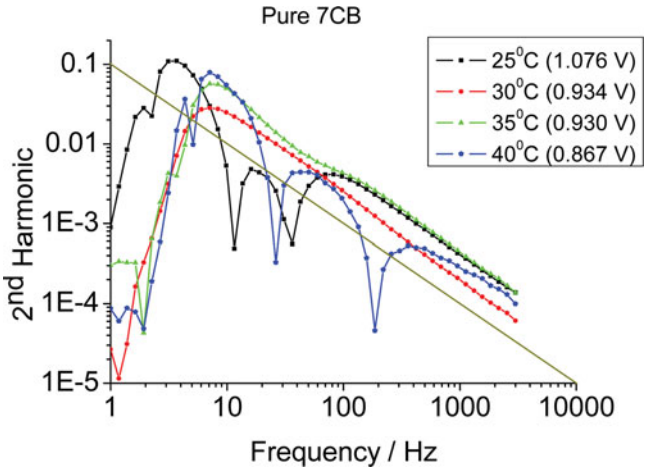

Figure 5. Amplitude of the 2nd harmonic modulation of the transmitted light through a planar nematic layer of pure 7CB vs. frequency. Experimental conditions same as on Figure 4. AC voltage amplitudes at various temperatures are selected at the points of maximum slope of the initial part of the transmittance vs. voltage curves (Figure 4). The straight line demonstrates an overall ω^{-1} slope of the 2nd harmonic spectrum.

3.4. Pure 7CB: Frequency spectrum of the 2nd harmonic

When AC voltage is used to drive the Freedericksz transition in a planar nematic layer of positive dielectric anisotropy, the theory predicts that the average tilt value of the layer will correspond to that with a DC voltage having the effective rms value of the AC one, and it will be weakly modulated with 2nd harmonic of the driving frequency [19]. The modulation amplitude vs. frequency is expected to scale like ω^{-1}.

Figure 5 demonstrates the 2nd harmonic frequency spectra of 7CB at several temperatures on a log-log scale. The drastic amplitude decrease below 10 Hz is possibly due to the charge screening of the internal field at very low frequencies. Apart from some outliers, the overall slopes of the spectra in 10 – 3000 Hz range are seen to be indeed proportional to $\omega^{-1,}$ as compared to the straight line (on a log-log scale) with the ω^{-1} slope.

3.5. Nanofilled 7CB + 3%A300: Amplitude Curves and Transients

The electro-optical curves of planar nanofilled nematic layers of 7CB+3%A300 also demonstrate a Freedericksz-like transition from opaque to transparent state of the cells, but at much higher threshold voltages (see Figures 6 and 7). The transmittance curves on Figure 6 are sigmoidal, unlike oscillating birefringence curves of pure 7CB in crossed polars on Figure 4. The curve at 41.26°C corresponds to isotropic phase, as one can judge from polarizing microscopic images. It displays a high transmittance that is voltage-independent. The curve at 40.4°C is just below nematic-isotropic phase transition and is almost voltage independent. Some discrepancy of Mettler transition temperatures (Figure 6) with DSC ones (Table 1) may be attributed to a difference in calibration of both instruments.

The transients of cell transmittance show that under present experimental conditions (hydrophilic surface of nanoparticles, relatively low density of nanoparticles, planar treatment of cell electrodes) the electro-optic response of our cells is monostable, and the

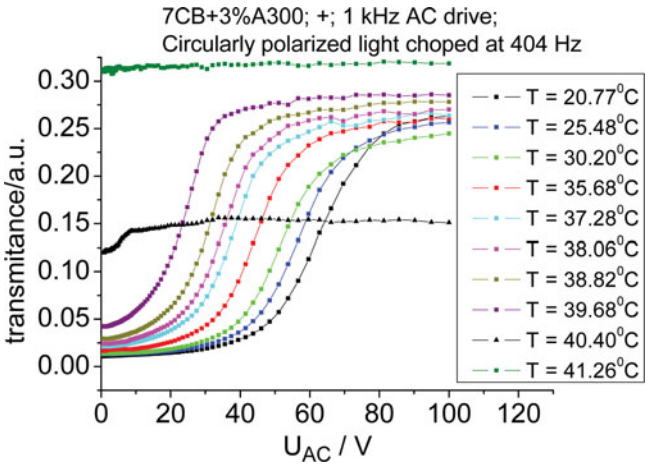

Figure 6. Transmittance vs. voltage curves of nanofilled 7CB+3%A300, demonstrating the temperature dependence of the Freedericksz threshold (as shown on Figure 7). AC driving voltage of 1kHz. Circularly polarized light, choped at 404 Hz, no analyser.

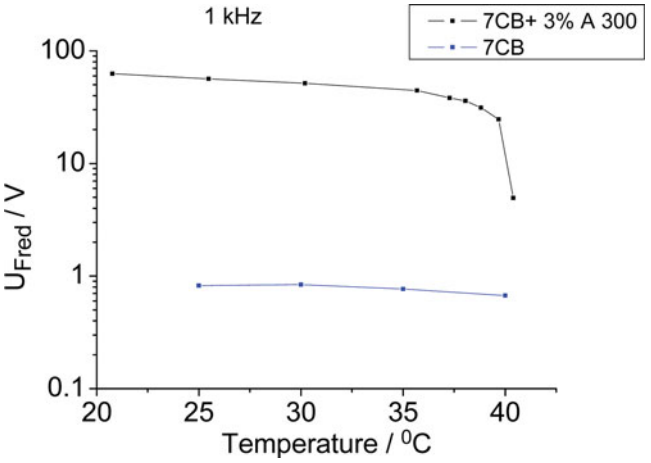

Figure 7. Comparison of Freedericksz thresholds of pure and nanofilled 7CB vs. temperature. Threshold voltages are obtained by extrapolation of the steepest parts of the transmittance curves to initial, zero voltage transmittance.

Table 1. Transition temperatures and thermal parameter for pure and nanofilled 7CB determined from DSC

		7CB		7CB + 3% A300	
		Heating	Cooling	Heating	Cooling
Transition temperature (°C)	Main peak	42.47	42.35	42.05	41.9
	Additional peak	—	—	41.98	41.84
ΔH (J/g) for main peak		1.87	1.95	1.61	1.66

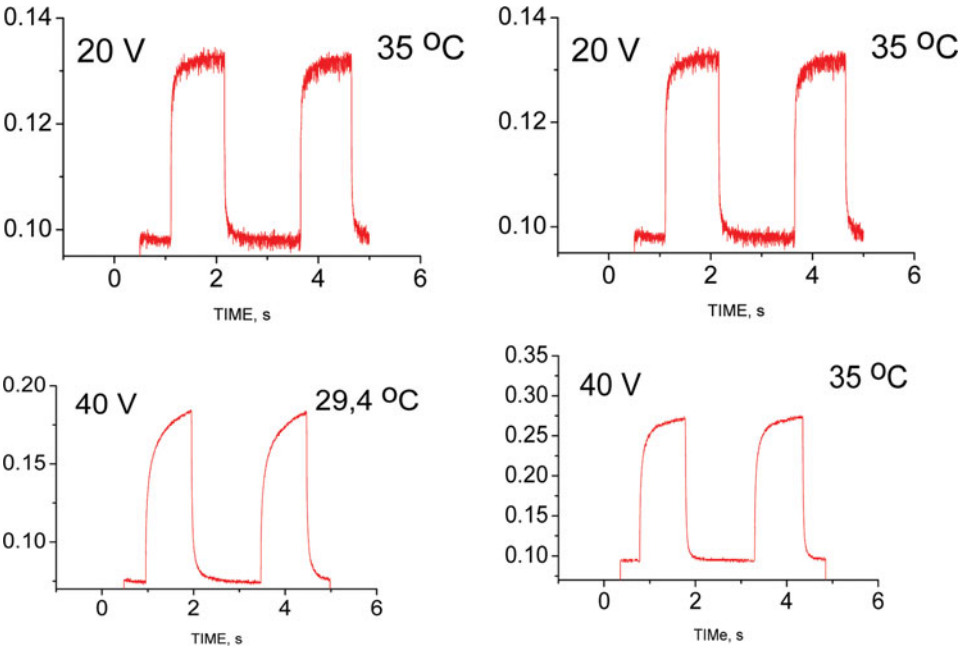

Figure 8. Transmittance transients of nanofilled cells in response to pulses of voltage (1 kHz wave packets) of variable amplitude at various temperatures.

scattering field-off state is reversible. The field-off relaxation is characterized by at least two relaxation times, a short (*ca.* ten miliseconds) and a long (*ca.* hundred miliseconds) one, differing by one order of magnitude (see Figure 9). For comparison, the field-off transients of pure 7CB cells are single exponents, and the relaxation time matches roughly the long relaxation time of nanofilled cells (80 ms at 35°C).

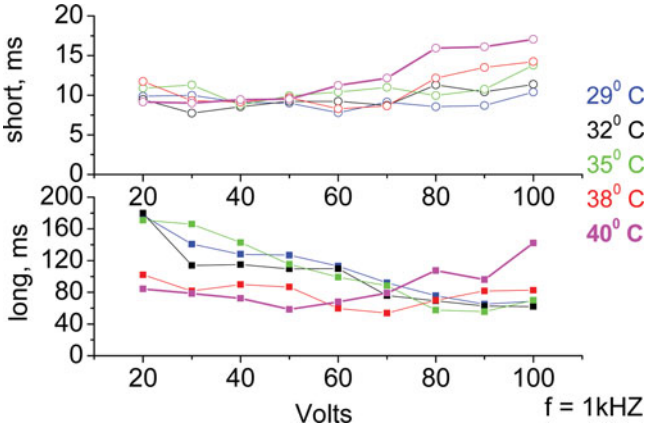

Figure 9. Short and long relaxation times of field-off transients

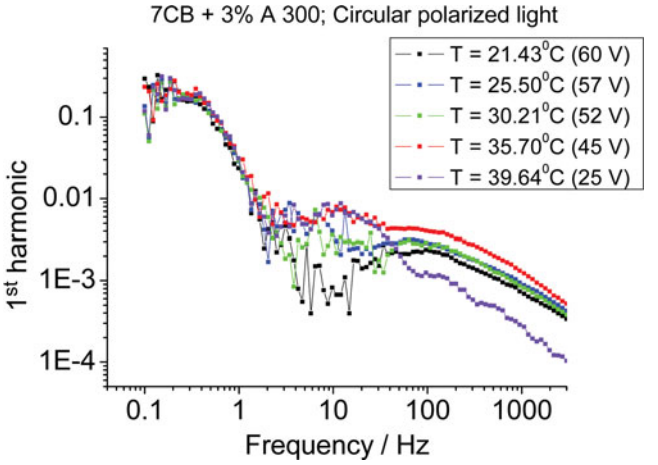

Figure 10. Amplitude of 1st harmonic vs. frequency

3.6. Frequency spectra of 1st and 2nd harmonics

Spectra were recorded according to the established procedure [1,2]. The amplitude of the AC driving signal at each temperature was chosen at the steepest point of transmittance vs. voltage curves (in Figure 6), as indicated in the insets of Figures 10 to 13. While 1st harmonic spectrum displays a complex shape, with two separate smooth frequency ranges and a noisy erratic region between them, the 2nd harmonic displays a broad, stable and only weakly frequency dependent modulation range. This is to be contrasted with the inverse frequency decay of the spectrum of the pure 7CB cell (Figure 5).

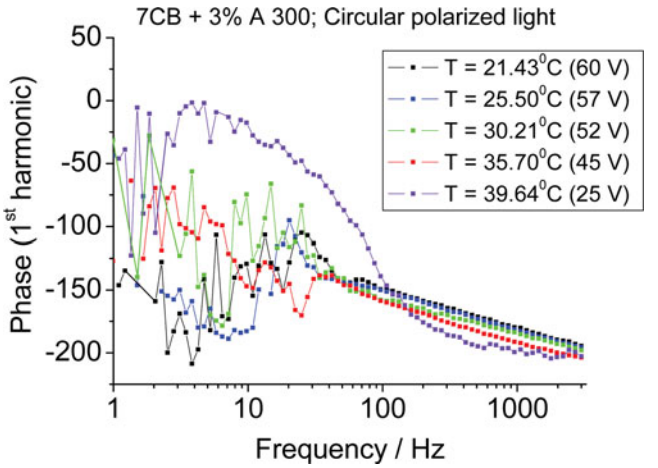

Figure 11. Phase of 1st harmonic vs. frequency

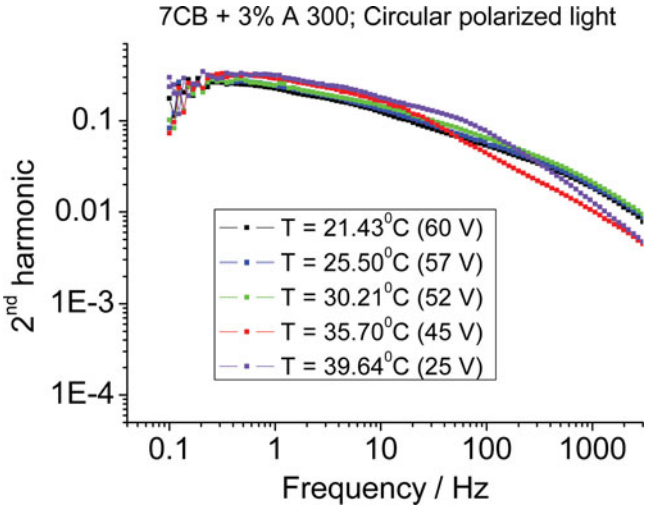

Figure 12. Amplitude of 2nd harmonic vs. frequency

4. Discussion

The finding of two phase transition temperatures (Table 1) motivates us to advance a two subsystems model for interpretation of electro optics of nanofilled nematics: a coexistence of entangled bulk-like domains (of average domain size d_B) and nano-disordered domains (average domain size d_N). Presumably, hydrophilic nanospheres of aerosil are concentrated in nano-disordered domains, provoking local gradients of nematic director that extend to the bulk region as well because of the collective properties of the nematic.

The size of bulk domains could be evaluated based upon comparison of Freedericksz thresholds in pure and nanofilled samples (Figure 7). Under a provisional assumption that splay elastic constants and dielectric anisotropy of pure nematic and bulk domains are the

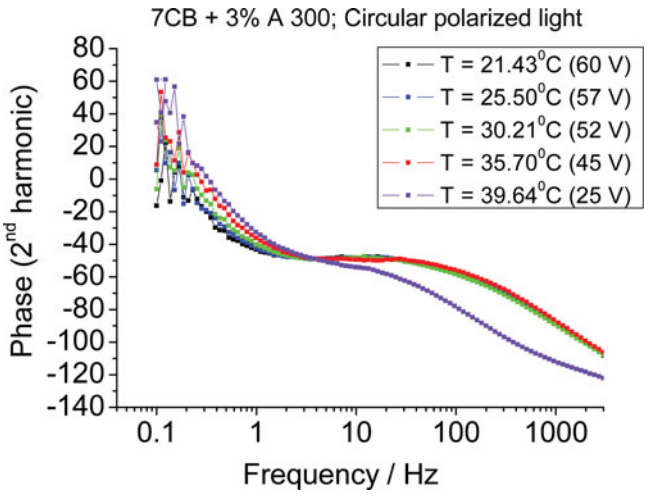

Figure 13. Phase of 2nd harmonic vs. frequency

same, and considering bulk domains as layers of thickness d_B, undergoing a Freedericksz-like transition at threshold voltage ${U_F}^B$, we could write:

$$ {U_F}^B / U_F = d/d_B $$

Consequently, at 29.5°C and $d = 25\ \mu$m, with $U_F = 0.9$ V and ${U_F}^B = 39.7$ V (Figure 7) we obtain $d_B = 567$ nm. Data in Figure 7 also tell us that this bulk domain size grows steeply by approaching N-I phase transition temperature; e.g. at 40.4°C, with $U_F = 0.67$ V and ${U_F}^B = 4.93$ V we obtain $d_B = 3.4\ \mu$m.

Similarly, the finding of two field-off relaxation times in nanofilled nematic layers, inferred from fitting field-off decay curves on Figure 8, one short (about 12 ms) and one longer (about 200 ms), prompted us to ascribe the short relaxation time to nano-disordered domains (τ_{N}), and the longer one to the bulk-like domains (τ_{B}). In general, field-off relaxation times of thin nematic layers scale like square of the layer thickness. Therefore, in even more rough assumption than above, i.e. that splay elastic constant and rotational viscosity of both regions do not differ, we could write:

$$ d_N / d_B = \sqrt{\tau_N / \tau_B} $$

Consequently, at 29.5°C, we would have:

$$ d_N \ = \ 567\ nm \sqrt{9.2\ ms / 110\ ms} = \ 164\ nm $$

Incidentally, two frequency ranges of first harmonic spectrum could also be identified: a lower frequency ($1/\tau_B = 9$ Hz) and higher frequency ($1/\tau_N = 110$ Hz) range. In general, the observation of a first harmonic in the nanostructured nematic (unlike in the pure one) can only be due to a gradient flexoelectric effect induced by gradient in the director orientation [20]. The identification of two ranges in the 1st harmonic amplitude spectrum points to a difference in the director gradients in the bulk and nanostructured regions. The phase spectrum is very unstable and noisy in the low frequency range, while becoming stabilized in the high frequency one.

5. Conclusion

Nanoconfined nematic/aerosil system displays interesting electrooptical properties, e.g. broad frequency range of 2nd harmonic light modulation. Flexo-dielectro-optical spectroscopy is demonstrated to be a powerful method to evaluate nanostructural parameters of filled nematics by macroscopic measurements.

Funding

Work supported partially by Bulgarian-Indian joint project DNTS/In 01/04 and by DFNI-TO2/18 grant. ILCC participation supported by 7FP REGPOT INERA 316309 project.

References

[1] Marinov, Y., Shonova, N., Versace, C. & Petrov, A.G. (1999). *Mol. Cryst. Liq. Cryst.*, *329*, 533.
[2] Petrov, A. G., Marinov, Y., D'Elia, S., Marino, S., Versace, C. & Scaramuzza, N. (2007). *J. Optoelec. Adv. Mat., 9*, 420.
[3] Iannacchione, G. S. (2004). *Fluid Phase Equilib., 17*, 222

[4] Iannacchione, G. S., Garland, C. W., Mang, J. T. & Rieker T. P. (1998). *Phys. Rev. E*, *58*, 5966.
[5] Prasad Bapat, N., Shankar Rao, D. S. & Krishna Prasad, S. (2009). *Thermochimica Acta., 495*, 115-119
[6] Marinelli, M., Ghosh, A. K. & Mercuri, F. (2001). *Phys. Rev. E*, *63*, 061713-1-9
[7] Kutnjak, Z., Kralj, S. & Zumer, S. (2002). *Phys. Rev. E 66. 041702-1-8*, Zakharov, A. V. & Thoen, J. (2004). *Phys. Rev. E, 69*. 011704-1-5.
[8] Roshi, A., Iannacchione, G S., Clegg, P. S. & Birgeneau, R.J. (2004). *Phys. Rev. E, 69* 031703-1-11.
[9] Bellini, T., Clark, N. A., Degiorgio, V., Mantegazza, F. & Natale, G. (2000). *Phys. Rev. E*, *57*, 2996.
[10] Jin, T. & Finotello, D. (2001). *Phys. Rev. Lett., 86*, 818.
[11] Lobo, C. V., Prasad, S. K. & Yelamaggad, C. V. (2006). *J. Phys.: Condens. Matter, 18*, 767.
[12] Bandyopadhyay, R., Liang, D., Colby, R. H., Harden, J. L. & Leheny, R. L. (2005). *Phys. Rev. Lett., 94*, 107801-1-4.
[13] Jayalakshmi, V., Geetha Nair G. & Prasad, S. K. (2007). *J. Phys.: Condens. Matter, 19*, 226213-1-12.
[14] Eidenschink, R. & de Jeu, W. H. (1991). *Electron. Lett., 27*, 1195.
[15] Puchkovskaya, G. A., Reznikov, Yu. A., Yakubov, A. A., Yaroshuchuk, O. V. & Glushchenko, A. V. (1996). *J. Mol. Struct., 381*, 133.
[16] Popa-Nita, V., Gerlic, I. & Kralj, S. (2009). *Int. J. Mol. Sci., 10*, 3971–4008.
[17] Caggioni, M. *et al.* (2004). *Phys. Rev. Lett.*, *93*, 127801
[18] (a) Geetha Nair et al. (2010). *J. Phys. Chem. B, 114*, 697 18; (b) Krishna Prasad, S., Sandhya, K.L., Nair, Geetha G., Hiremath, Uma S., Yelamaggad, C.V. & Sampath, S. (2006). *Liquid Crystals, 33*, 1121; (c) Krishna Prasad, S., Vijay Kumar, M., Shilpa, T. & Yelamaggad, C.V. (2014). *RSC Adv., 4*, *4453*.
[19] Pikin, S. A. (1981). *Strukturnie Prevrashcheniya v Zhidkih Kristallakh*, Nauka: Moscow (Eq. 6.42, p. 201).
[20] Petrov, A. G. (2001). In: *Physical Properties of Liquid Crystals, EMIS Datareviews Series*, Inst. Electrical Engineers, UK, vol. 25, 251–264.